Carbohydrate Polymers 75 (2009) 39–43

Contents lists available at ScienceDirect

Carbohydrate Polymers

journal homepage: www.elsevier.com/locate/carbpol

Composition and structure study of natural *Nelumbo nucifera* fiber

Di Liu, Guangting Han *, Jiancheng Huang, Yuanming Zhang

Laboratory of New Fiber Materials and Modern Textile, The Growing Base for State Key Laboratory, Qingdao University, Qingdao 266071, PR China

ARTICLE INFO

Article history:
Received 21 March 2008
Received in revised form 1 June 2008
Accepted 2 June 2008
Available online 8 June 2008

Keywords:
Nelumbo nucifera
Morphologic structure
Fibril
Natural fiber

ABSTRACT

Nelumbo nucifera (*Nn.*) fiber is the isolated secondary wall of the *Nn.* leafstalk Tracheary elements which has a unique shape. As the shape of the fiber may strongly affect the industrial uses especially for textile usage, the morphology and structure of *Nn.* fiber at different growth stages were investigated by several techniques in the present work. The *Nn.* fiber has spriral morphology with cellulose I structure. The diameter of mature fiber is about 4 μm and the cross-section shows elliptical or slightly oval shape without lumen. These findings aim to deeply understand the structure of *Nn.* fiber which is expected to be helpful to bring *Nn.* fiber into industrial use.

1. Introduction

Today, with the enhancement of people's consciousness on environment problems and the demand of environment-friendly fabric, natural fibers have received a great deal of attention due to their great importance of "green" and health protection properties and have been widely used in many fields, such as textile industry and daily life (Mohanty, Misra, & Drzal, 2005; Netravali & Chabba, 2003). It has become a significant topic to exploit and study new natural resource that is green and environment-benignly. *Nelumbo nucifera* has extensive cultivation in China, and the *Nn.* root is usually considered as an ornamental or as an appetizing food due to its low content of the fibers, while *Nn.* leafstalk contains more fiber and is easy to obtain. Although some researches about the *Nn.* leafstalk and *Nn.* root have been reported, little attention has been paid on the systematical study of *Nn.* fiber. *Nn.* fiber usually can be extracted from *Nn.* leafstalk, which is a kind of new natural fiber and will have broad space for development because the *Nn.* has great advantage of simple cultivation techniques, abundant resources and low costs, etc. (Murali Mohan Rao & Mohana Rao, 2007). The systematical research on the *Nn.* fiber may help to further exploit the applications, which can be an interesting income for lotus producers and for a regional economy (Oliveira, Cordeiro, Evtuguin, Torres, & Silvestre, 2007).

Although the morphology of *Nn.* fiber has been studied previously, the research has been only limited to one period, the structures of *Nn.* fiber in different periods and the ultrastructure of *Nn.* fiber have not been studied yet (Chen, Zhang, & Yan, 1980; Sun, Wang, Zhang, & Zhang, 1998; Wang, 1957; Zeng, 1992). In this paper, the composition and morphologies of *Nn.* fiber in different periods and the growing regulation of the morphologic structure of *Nn.* fiber are studied carefully and the ultrastructure of *Nn.* fiber is investigated by TEM.

2. Experimental

2.1. Material

Nn. leaf is the organ for gas exchanging and producing nutrition by photosynthesis. It experiences a series of growth stages from floating on the water to playing an important role. Vascular bundle gradually becomes to mature as the leaf develops. In this paper, the leaves are divided into four growth stages and the corresponding standard is shown in Table 1. By this means, the morphology changes of the fiber at different stages can be well investigated.

The *Nn.* leafstalks are got from the World of Water Lily in Laoshan district of Qingdao city (China). The leafstalks are chosen according to the stages defined in Table 1 and all leafstalks are from the only kind of *Nn.* named Bright Red Bowl.

2.2. Fiber production

The Tracheary elements were extracted from the leafstalks which were dipped into water with the airtight container for 30 days at room temperature and dried naturally.

The Nn. fibers were extracted from the leafstalks of different growing stages by hand with knives and tweezers.

The Lotus root fibers were extracted from the lotus root with the same method as the *Nn.* fiber.

The Petioles were the leafstalks dried naturally.

* Corresponding author. Tel.: +86 532 85952787; fax: +86 532 85953148.
E-mail address: kychgt@qdu.edu.cn (G. Han).

0144-8617/$ - see front matter © 2008 Elsevier Ltd. All rights reserved.
doi:10.1016/j.carbpol.2008.06.003

Table 1
Dividing standard for leaves

Stage	Name	Standard
1	Cataphyll	The distance of leaf and water is less than 50 cm, the leaf is wrapping tightly, there is hardly any spines on the leafstalk with tender handle
2	Primary expanding	Leaf expanding to brink wrapping, few spines on the leafstalk with tender handle
3	Expanding	Expanding, thin leaf, spines on the leafstalk are not acuate and straight
4	Function metaphase	Completely expanded, the leaf becomes thicker with waxy handle and dark colour and lustre, spines on the leafstalk are hard and straight

2.3. X-ray diffraction

The *Nn.* fiber, Tracheary elements and Petioles were used for X-ray diffraction measurements, respectively. The three samples were ground in a Wiley mill and all the powders were then screened by 60 meshes prior to pressing. X-ray diffraction patterns (XRD) were recorded on a Bruker D8 Advance X-ray diffractometer using a Cu K_α source ($\lambda = 0.154178$ nm).

2.4. FT-IR spectroscopy

Fourier Transform-Infrared spectra of four different samples, *Nn.* fiber at the first stage (Fiber 1), *Nn.* fiber at the fourth stage (Fiber 4), the Tracheary elements as well as Petioles were measured by a Nicolet Centaurus IR-Microscope and the spectra were obtained with an accumulation of 32 scans and with a resolution of 2 cm^{-1}. In order to obtain good resolution spectra it is necessary to mill the *Nn.* fiber to an average length of 0.2 mm. The milled fibers were mixed with an analytical grade KBr and then the mixture was pressed into a disk for the FT-IR measurements.

2.5. Scanning electron microscopy (SEM)

Longitudinal shape of the *Nn.* fiber was observed after sticking the *Nn.* fibers as parallel as possible on the two-sided sticky glue, which has been stuck on the microscope slide.

To observe the cross-section, the fiber was sliced with Y-172 microtome beforehand. In order to slice up more effectively, the fiber was covered by two-sided sticky glue in proper size instead of celloidin. And then the cross-section of the fiber was stuck on the microscope slide for observing.

To get a deep understanding of the fiber's microstructure, the fracture morphology after embedding was also studied by SEM. Firstly, the *Nn.* fiber was saturated with 2.5% glutaric dialdehyde for 2 h at room temperature and then washed with 0.1 mol/L phosphoric acid buffer solution (PBS, pH 7.3–7.4) for 1 h. Secondly, the fiber was soaked with 1% perosmic acid for 1 h and then washed with PBS again for 20 min. Thirdly, the dehydration was carried out in certain gradient: 70% acetone for 15 min, 80% acetone for 15 min, 90% acetone for 15 min, 100% acetone for 10 min (twice). Fourthly, the fiber was embedded in epoxy resin and heated up in the drying oven for 12 h at 45 °C and subsequently for 36 h at 60 °C. In this way, the epoxy resin would polymerize and form the embedding block. Finally, the embedding block was put into liquid nitrogen for 15–20 s, and then was broke off into two pieces with pliers for observation of microstructure of the cross-section.

The SEM images of the samples were examined using a JEOL JSM-6390LV microscope. Prior to the analysis, the samples were coated with gold (layer thickness ~30 nm, time 15–20 min) to avoid sample charging under the electron beam.

2.6. Transmission electron microscope (TEM)

Two different fibers, *Nn.* fiber and Lotus root fiber, were used for TEM measurements. The two samples were boiled twice in excessive 1% NaOH solution for 3 h. Then, after 12 h, the samples were put into 0.05 mol/L HCl solution and washed with distilled water. Suspending liquid was got after the fibers putting in the distilled water for 4 h with the supersonic. For sample preparation, the copper net is used and the TEM images were examined by a JEOL JEM-1200EX microscope.

3. Results and discussion

3.1. X-ray diffraction (XRD) study

To investigate the crystal structures of the as-prepared *Nn.* Fiber, Tracheary elements and Petiole, The XRD patterns were measured for these samples. Fig. 1 shows their corresponding wide-angle XRD patterns. It can be seen that all the samples show cellulose I structure (Dyer & Daul, 1985) with the diffraction peaks of the 2θ angles at 16.3°, 22.2°, 34.9°, which were assigned to $(10\bar{1})$, (002) and (040) planes, respectively. And from the XRD patterns, it can be known that the crystal structure was well-reserved during the fiber preparation.

3.2. FTIR study

As a powerful method, FTIR spectroscopy has been widely used in cellulose research, from which the direct structural information or any changes can be obtained (Wang, Han, & Zhang, 2007). Fig. 2 shows the FTIR spectra of four samples: *Nn.* fiber at the first stage (Fiber 1), *Nn.* fiber at the fourth stage (Fiber 4), the Tracheary elements as well as Petioles. It can be seen that the FTIR spectra did not change largely for these samples except the relative intensity of the absorption bands. The absorption bands at 3361 cm^{-1} and 2900 cm^{-1} appeared, which can be ascribed to O—H or N—H stretching vibrations and CH and CH_2 stretching vibrations (Silverstein & Webster, 1998), respectively. The vibration peak at 1734 cm^{-1} in the spectrum is ascribed to the C=O stretching of

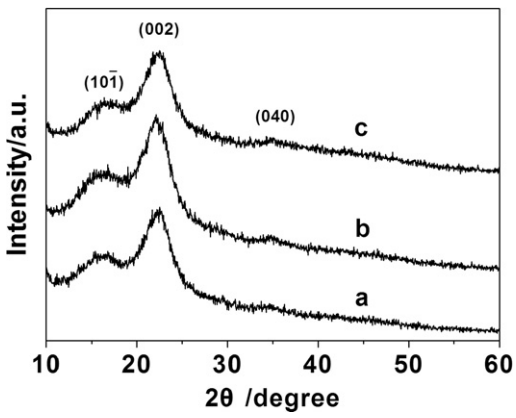

Fig. 1. The XRD patterns of the samples: a, *Nn.* fiber; b, Tracheary elements; c, Petiole (Di Liu, Guangting Han, Jiancheng Huang, Yuanming Zhang).

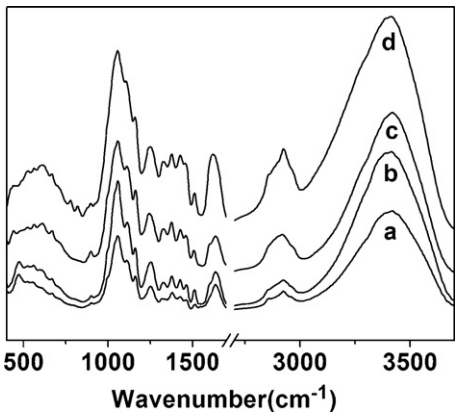

Fig. 2. The FTIR spectra of the four samples: a, Fiber 1; b, Fiber 4; c, Tracheary elements; d, Petiole (Di Liu, Guangting Han, Jiancheng Huang, Yuanming Zhang).

methyl ester and carboxylic acid in pectin or the acetyl group in hemicelluloses. The strong absorption peak of 1033 cm^{-1} is attributed to C—O stretching vibrations which belongs to polysaccharide in cellulose (Xie, Chang, & Wang, 2001). The absorption band at 1640 cm^{-1} is assigned to oxygenous group in lignin.

3.3. SEM study of the fibers

3.3.1. Longitudinal shape

As the *Nn.* is a kind of perennial water plant with long Petiole, in this paper, the *Nn.* fiber refers to the thick secondary wall, which is the layer adhered to the internal surface of the primary wall after cell volume stop increasing. Petiole Tracheary element is a general designation of vessel and tracheid.

By longitudinal observation, the fibers showed a kind of spiral structure (Fig. 3A). This structure can well reflect the arrangement of the *Nn.* Fiber in Tracheary element. From Fig. 3, it can be seen that the number of the fiber in the spiral structure usually ranges between 6 and 12. The surface of *Nn.* fiber is not extremely smooth in nature as some knots like drip wax appears on the surface at intervals of 15–25 μm. Most of the *Nn.* fibers do not compose to spiral structure separately but with some conglutinations existing between the single fiber. And even more interesting, all the conglutinations only appear on one side (outside of the screw) of the fiber.

The *Nn.* fiber displays a certain rule of growth in different growing periods. First, the outward appearance of the fiber shows different characteristics at four stages (Fig. 3). There are no links between the fibers at the first stage (Fig. 3A, Cataphyll), so the fibers are arranged isolated. From the second stage (Fig. 3B, Primary expanding) the links appear gradually with a small quantity and irregularly. From the third (Fig. 3C, Expanding) to the fourth (Fig. 3D Function metaphase) stage, the quantity of the links between the fibers increases obviously and more regularly. The links are arranged at intervals of about 20 μm (Fig. 3D) and this is almost the same as the distance between the drip wax that appear on the surface. Thus, the drip wax appears in the first period is probably the rudiment of the link. Second, the change of the diameter uniformity of the fiber in different growing period of the leaf is distinct. The Fig. 4 demonstrates the changes of the diameter uniformity of four stages. At the first stage, the fiber is at the preliminary phases of growth and displays a gourdshaped appearance. The concave–convex rule is so clear that the diameter uniformity is bad. Along with the maturity of the leaf, the diameter uniformity improves gradually and the concave–convex degree decreases evidently. At the fourth stage, along with the leaf reaches the maturity on the whole, the diameter uniformity is good and the *Nn.* fiber tends to become even with no obvious gourdshaped appearance.

Furthermore, statistical analysis and account of the fiber diameter are carried out due to the different situation of four stages and 30 data are chosen from concave and convex section of each phase, respectively. The numerical values of average diameter obtained are shown in Table 2. It can be found that the fiber diameter is increasing in a mess with the leaf gradually reaching to maturity but the increasing scope of each period is different. The value of Convex/Concave can display the level of uniformity of diameter. The uniformity is becoming better as the ratio grows larger, and

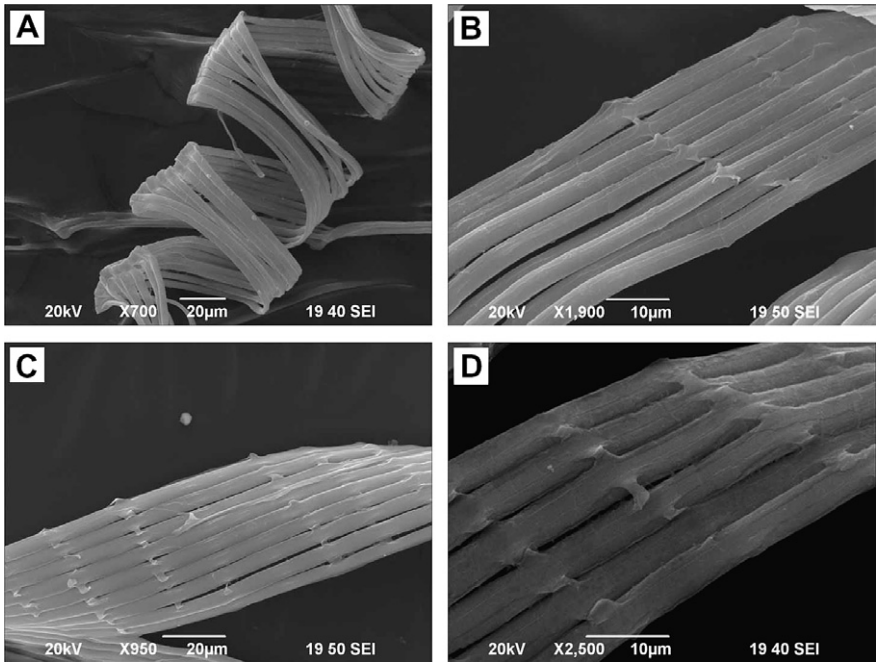

Fig. 3. SEM imges of the longitudinal shape of *Nn.* fiber at different stages: (A) Cataphyll (B) Primary expanding (C) Expanding (D) Function metaphase (Di Liu, Guangting Han, Jiancheng Huang, Yuanming Zhang).

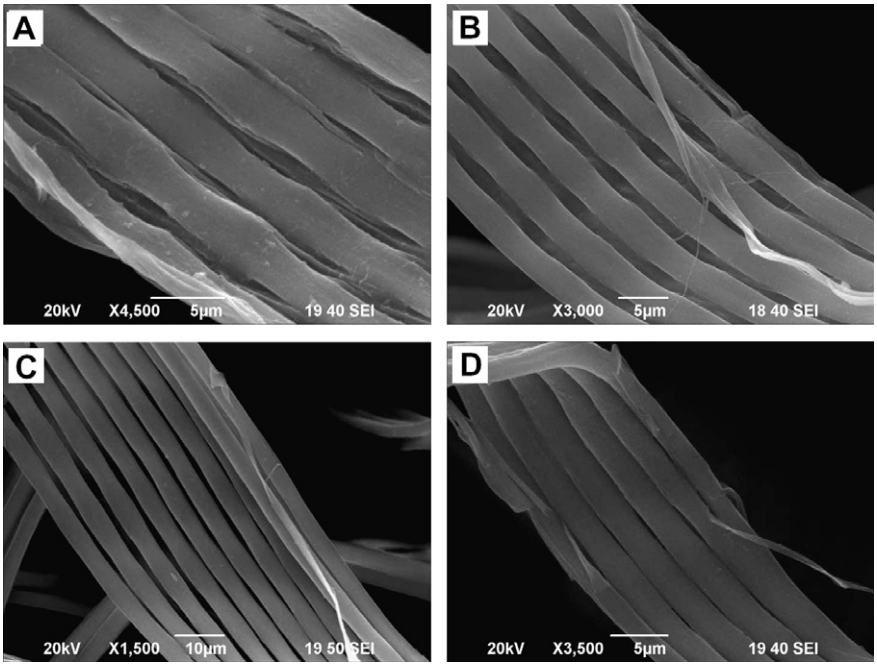

Fig. 4. SEM images of characteristics of diameter of *Nn.* fiber at different stages: (A) Cataphyll, (B) Primary expanding, (C) Expanding, (D) Function metaphase (Di Liu, Guangting Han, Jiancheng Huang, Yuanming Zhang).

Table 2
Statistics of fiber diameter

Stage	Concave diameter (μm)	Convex diameter (μm)	Convex/concave
Cataphyll	3.36	3.78	0.888
Primary expanding	3.48	3.91	0.891
Expanding	3.67	4.09	0.895
Function metaphase	3.84	4.11	0.933

vice versa. The conclusion is in accord well with the longitudinal view of the fiber.

3.3.2. Cross-sectional observation

Elliptical or slightly oval shape of unattached *Nn.* fiber is shown in Fig. 5A. The fiber was solid with no central canal or lumen like other natural plant fibers as cotton or linen fibers and much thinner than other natural fibers with the diameter is only 3–5 μm. Some sections are connected because of the conglutination that exists between the fibers.

Some biggish slit hole and small cluster are presented on the cross-brittle fracture surface of *Nn.* fiber which is displayed in Fig. 5B. They are probably some interior structural unit of fiber due to their ubiquity on the section. But even with the slit hole and small cluster, the region outside which that was relative stable and compact shows elliptical like or slightly oval shape. The bunchy structure may be due to the torsion and extraction of interior structure unit in the process of brittle fracture. And this can also indicate that the interior structure units with different degree of denseness and intensity. The aperture and hole inside of the fiber could therefore affect the absorbent quality and the warmth retention property of the fiber obtained.

3.3.3. Microstructure

There are several levels of microstructure in the growing process of the fiber. It includes ranks of single macromolecule, elementary fibril, microfibril, fibril, macrofibril and fiber. However, the microstructure of fibers in different species and different breeds is varied and sometimes does not include every rank (Wang, Jiang, & Li, 2004). The ultrastructure of the longitudinal brittle fracture surface of *Nn.* fiber is shown in Fig. 6. Bundles of microfibril in parallel and some microfibril (about 50 nm) comprising wide fibrils (about 200 nm) are observed. It can be confirmed that the microfibril is the fibril of *Nn.* fiber and the wide fibrils

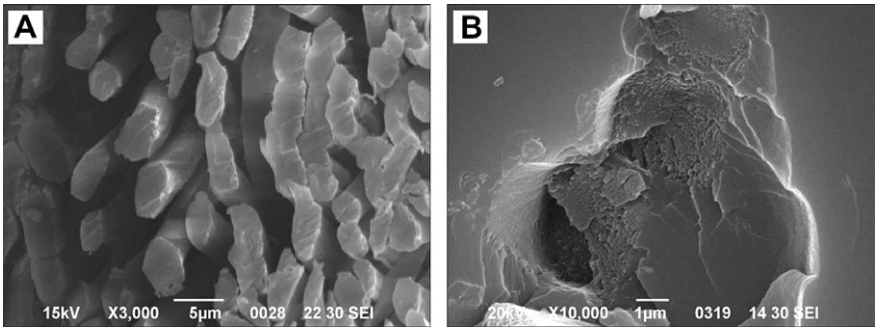

Fig. 5. The SEM images of cross-section (A) and cross-fracture surface of *Nn.* fiber (B) (Di Liu, Guangting Han, Jiancheng Huang, Yuanming Zhang).

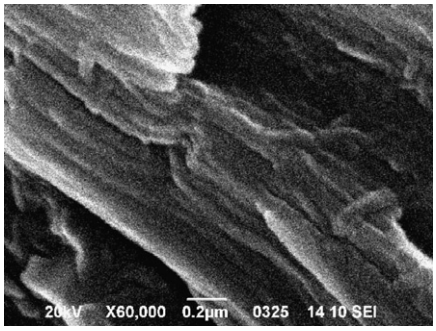

Fig. 6. The high-magnification SEM image of *Nn.* fiber. (Di Liu, Guangting Han, Jiancheng Huang, Yuanming Zhang).

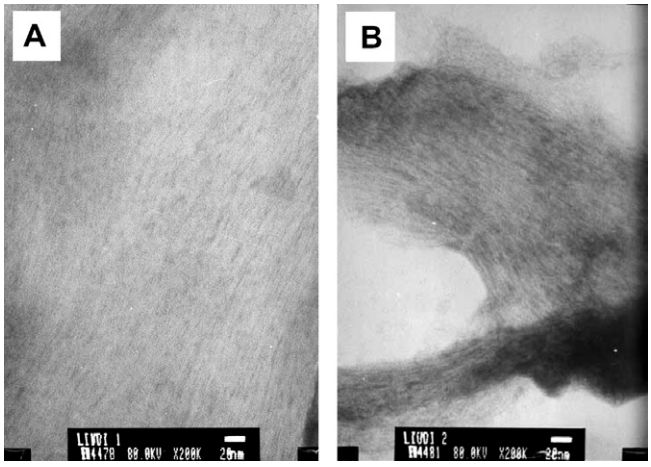

Fig. 7. TEM images of the two fibers: *Nn.* fiber (A) and Lotus root fiber (B). (Di Liu, Guangting Han, Jiancheng Huang, Yuanming Zhang).

bunch is the macrofibril of *Nn.* fiber. The arrangement of the fibril is more compact than which of the macrofibril. The interior connection of the macrofibril are mainly by fibrils and molecular chain (Ou, Jiang, & Li, 2005).

3.4. TEM study of natural fibers

To further study the microstructure of these natural fibers, *Nn.* fiber and Lotus root fiber are selected for investigation. Fig. 7 shows the TEM images of the *Nn.* fiber and Lotus root fiber. It can be seen that the arrangements of microfibrils of *Nn.* fiber is more orderly that that of the Lotus root fiber, in which the width of the microfibrils is about 0.5–1.5 nm. Furthermore, the microfibrils of *Nn.* fiber have longer lengths than those of the Lotus root fiber, indicating that the *Nn.* fiber may be used directly in the industries.

4. Conclusion

The experimental results show that *Nn.* fiber displays a spiral morphology, which shows cellulose I structure. The longitudinal shape of the fiber is smooth and the diameter of the fiber is increasing irregularly and becomes uniform with the leaf gradually reaching to maturity. The average diameter of the mature fiber is about 4 μm and cross-conglutinations appeared between the fibers at intervals of 20 μm which is the same as the distance of the drip wax on the surface. Cross-sectional observation of *Nn.* fiber shows elliptical or slightly oval shape with no lumen. The results also show that the *Nn.* fiber is composed of well organized microfibrils and the arrangement of the fibril is more compact than that of the Lotus root fiber.

Acknowledgements

This work was supported by the National Natural Science Foundation of China (No. 50573035) Provincial Key Sci-Tech Special Projects of Shandong Province in China (2006GG1103088). The authors are very grateful to Prof. Yongjun Sun at Qingdao University, for his kind help. We also thank Dr. Peizhi Guo at Qingdao University for helpful discussions.

References

Chen, W. P., Zhang, S. M., & Yan, S. Z. (1980). *Journal of Nanjing Teachers College, 4*, 64–70.
Dyer, J., & Daul, G. C. (1985). Rayon fibers. In M. Lewin & E. M. Pearce (Eds.), *Handbook of fiber science and technology. Fiber chemistry*. New York: Marcel Dekker.
Mohanty, A. K., Misra, M., & Drzal, L. T. (2005). *Natural fibers, bioploymers, and biocomposites*. Boca Raton: CRC press.
Murali Mohan Rao, K., & Mohana Rao, K. (2007). *Composite Structures, 77*, 288–295.
Netravali, A. N., & Chabba, S. (2003). *Mater Today, 6*, 9–22.
Oliveira, L., Cordeiro, N., Evtuguin, D. V., Torres, I. C., & Silvestre, A. J. D. (2007). *Industrial Crops and Products, 26*, 163–172.
Ou, L., Jiang, L., & Li, J. (2005). *Journal of Textile Research, 26*, 45–46.
Silverstein, R. M., & Webster, F. X. (1998). *Spectrometric identification of organic compounds* (6th ed.). New York: Wiley.
Sun, J. H., Wang, J. Z., Zhang, Y. Z., & Zhang, J. Z. (1998). *Journal of Chinese Electron Microscopy Society, 17*, 114–118.
Wang, X. Q. (1957). *Bulletin of Biology*, 14–17.
Wang, L. L., Han, G. T., & Zhang, Y. M. (2007). *Carbohydrate Polymers, 69*, 391–397.
Wang, Y. H., Jiang, Y., & Li, F. Y. (2004). *Journal of Jilin Institute of Technology, 1*, 69–71.
Xie, J. X., Chang, J. B., & Wang, X. M. (2001). *Applications of FTIR in organic chemistry and pharmic chemistry.*, 77–78.
Zeng, X. F. (1992). *Journal of Biology*, 10–44.